

Large tunability of Néel temperature by growth-rate-induced cation inversion in Mn-ferrite nanoparticles

Aria Yang,¹ C. N. Chinnasamy,¹ J. M. Greneche,² Yajie Chen,¹ Soack D. Yoon,¹ Kailin Hsu,¹ C. Vittoria,¹ and V. G. Harris^{1,a)}

¹Department of Electrical and Computer Engineering, Center for Microwave Magnetic Materials and Integrated Circuits, Northeastern University, Boston, Massachusetts 02115, USA

²Laboratoire de Physique de l'Etat Condensé, UMR CNRS 6087, Université du Maine, 72085 Le Mans, Cedex 9, France

(Received 2 January 2009; accepted 21 February 2009; published online 18 March 2009)

The tuning of Néel temperature by greater than 100 K in nanoparticle Mn-ferrite was demonstrated by a growth-rate-induced cation inversion. Mn-ferrite nanoparticles, having diameters from 4 to 50 nm, were synthesized via coprecipitation synthesis. The Néel temperature (T_N) increased inversely to the cation inversion parameter, δ (i.e., defined as $(\text{Mn}_{1-\delta}\text{Fe}_\delta)^{\text{tet}}[\text{Mn}_\delta\text{Fe}_{2-\delta}]^{\text{oct}}\text{O}_4$). Concomitantly, T_N increased with increased particle growth rate and particle size. These results unambiguously establish cation inversion as the dominant mechanism in modifying the superexchange leading to enhanced T_N . The ability to tailor T_N enables greater flexibility in applying nanoparticle ferrites in emerging technologies. © 2009 American Institute of Physics.

[DOI: 10.1063/1.3099340]

Due to high magnetic permeability and low conduction losses, spinel ferrites find wide use in ultrahigh frequency applications. As nanoparticles (NPs), they are also considered for biomedical applications, including as contrast agents in magnetic resonance imaging¹ and in promising cancer remediation therapies such as targeted drug delivery, magnetohyperthermia, and magnetorheological fluids.² However, magnetic properties have been found to vary widely in ferrite NPs.^{3–5} In order to realize their full potential, understanding the processing and refinement of ferrite NPs is essential. One parameter of great importance is the Néel temperature (T_N). T_N derives from superexchange interactions that are sensitive to cation-anion-cation bond angles and cation type and valence. Demonstrating its importance is the application of ferrite NPs in oncological magnetohyperthermia; in this application the ability to tailor Néel temperature allows for flexibility in determining operational parameters, such as rf field strength, frequency, and targeted cell temperatures, leading to a higher efficacy in tumor cell necrosis.

In this letter, we address an important and controversial problem, that is, the influence of particle size on the Néel temperature, and other intrinsic magnetic properties, of ferrite NPs.^{6–14} Several studies have established a strong correlation between cation disorder, processing conditions, and magnetic properties,^{7,10–12,14,15} while others point to finite size scaling and surface spin structures as the dominant mechanism determining NP magnetism.^{6,8,9,13}

Mn-ferrite is chosen as the focus of this study since Mn ions are of comparable size to Fe ions and exist in a multitude of oxidation states, allowing them to readily substitute for Fe cations on tetrahedral and octahedral sites within the spinel ferrite lattice. Further, previous researchers studied Mn-ferrite NPs and, in particular, the size dependence of

some physical and magnetic properties,^{6–9,16–20} allowing us to evaluate our findings in both a historical and technical context.

The investigation of size effects of magnetic properties in ferrite NPs was first reported by Tang *et al.*⁶ in 1991, who measured an enhanced Néel temperature in Mn-ferrite prepared by chemical coprecipitation. In that report, the authors attributed this enhancement to finite size scaling. Shortly thereafter, van der Zaag *et al.*⁷ conjectured that the effect could be wholly attributed to cation redistribution, in which Mn cations fill a greater fraction of octahedral sites than similar materials prepared by more equilibrium processes. In 1992, Tang *et al.*¹⁶ revisited this problem and argued that a cation redistribution was insufficient to account for the measured rise in T_N . In 1994, Kulkarni *et al.*⁸ again attributed a rise in T_N of Mn-ferrite NPs to finite size scaling. Van der Zaag *et al.*²¹ countered that a nonequilibrium cation distribution, together with the oxidation of Mn^{2+} to Mn^{3+} , caused the rise in T_N . It is important to note that nearly all of these studies report the trend of increasing T_N with reduction in particle size. It is in this context that we propose to resolve the role of particle size and address the mechanism that gives rise to enhanced T_N in Mn-ferrite NPs as well as explore the control of this enhancement through processing.

The Mn-ferrite NPs of the present study were synthesized by a modified coprecipitation method, which entailed dissolving 0.1 M of iron (III) chloride hexahydrate ($\text{FeCl}_3 \cdot 6\text{H}_2\text{O}$, 99%, Sigma Aldrich) with 0.05 M of manganese (II) chloride ($\text{MnCl}_2 \cdot 4\text{H}_2\text{O}$, 99%, Sigma Aldrich) in distilled water at a ratio of $[\text{Fe}^{3+}]/[\text{Mn}^{2+}] = 2:1$ to maintain the stoichiometry. The mixed metal chloride precursor solution was introduced slowly into a boiling NaOH solution, and the reaction was carried out at 98 °C for 120 min. The pH value of the solution was adjusted by varying the molar amounts of $[\text{OH}^-]$ from 0.425 to 4.0 M. The pH environment is critical to particle nucleation, rate of growth, stabilization, and ultimately the size of the resulting particles. Following

^{a)}Electronic mail: harris@ece.neu.edu.

TABLE I. Short-range structure properties determined from EXAFS analyses of Mn-ferrite NP samples. The uncertainty in the least significant digit is included in parenthesis.

Average particle diameter by TEM	4 nm	7.5 nm	25 nm	50 nm	Ceramic standard ^a
Lattice parameter (nm)	0.8421(2)	0.8400(2)	0.8387(2)	0.8383(2)	0.85
Oxygen parameter (nm)	0.0388(2)	0.0387(2)	0.0387(1)	0.0385(1)	0.038 46
EXAFS <i>R</i> factors	0.024	0.027	0.027	0.020	...
Inversion parameter (%)	62.91 ± 1.84	57.83 ± 2.09	55.68 ± 1.74	51.07 ± 1.93	20

^aReference 22.

the completion of the reaction, the resulting particles were rinsed in distilled water, filtered, and dried at 70 °C for 12 h.

The NP samples were studied by x-ray absorption fine structure (XAFS) spectroscopy, x-ray diffraction (XRD), transmission electron microscopy (TEM), thermomagnetic measurements, and Mössbauer effect spectroscopy. Due to space constraints, a detailed discussion of the XAFS and thermomagnetic properties is presented here with other results eluded to as necessary to support and clarify data trends and relationships.

XRD analysis using Cu *K*α radiation indicated that all MnFe₂O₄ NP samples existed as pure phase spinel ferrite (space group: *Fd* $\bar{3}m$). By controlling the concentration of [OH⁻] in the processing solution, four batches of nearly monodispersed samples of different mean sizes were synthesized. Average particle diameters were estimated from Scherrer analysis and by direct TEM imaging to range from 4 to 50 nm. This information, together with the short-range structure and electronic properties acquired from the XAFS analysis, is presented in Table I. Chemical analysis of all NP samples, using induction coupled plasma spectrophotometry and energy dispersive x-ray analysis, confirmed the elemental composition ratio of Mn:Fe to be 0.5.

The temperature dependent magnetic properties were collected by vibrating sample magnetometry over a temperature range from 20 to 800 K in fields of up to 5000 Oe. Figure 1(a) shows the variation in magnetization with temperature for the 50 nm ferrite sample measured in a magnetic field of 1000 Oe. These data, representative of other NP samples, were fit to the Curie–Weiss molecular field approximation allowing for determination of the Néel temperature. Values of *T_N* for all NP samples are presented in Fig. 1(b) and were found to be higher than the ceramic standard (*T_N* = 573 K).²²

XAFS data, containing both the x-ray absorption near edge structure (XANES) and extended x-ray absorption fine structure (EXAFS) regions, were collected in a transmission geometry at room temperature at the National Synchrotron Light Source at Brookhaven National Laboratory using beam line X23B. Data were analyzed and modeled using the ATHENA and ARTEMIS codes developed by Ravel and Newville, respectively.²³ Cation distribution determined in ferrite materials by EXAFS was first reported by Harris *et al.*²⁴ and later extended to a multiedge refinement by Calvin *et al.*²⁵ Theoretical EXAFS standards were generated by the FEFF-6 codes of Rehr *et al.*²⁶ A constrained atomic model of the spinel ferrite²⁷ was employed in EXAFS analysis. The Fourier transformed EXAFS data were fit using the FEFF-generated EXAFS. The best fit and experimental data for the 7.5 nm sample are presented in Fig. 2(a). The quality of the

fit between experiment and modeled data [Fig. 2(a)] is representative of the best fit data for other samples as reflected by the statistical *R*-factor (Table I). From Table I, it is seen that all four samples have reduced lattice parameters in comparison to the bulk value²³ with the oxygen parameter dilated less than 1% relative to the bulk value. As particle size increased, the lattice parameter reduced continuously from 0.8421 to 0.8383 nm. As seen in the inset of Fig. 1(b), the degree of contraction is proportional to the increase in Néel temperature. We conjecture that the contraction of the lattice leads to greater cation-anion-cation bond angles and increased superexchange interactions.²⁸ In all four samples, the EXAFS modeling indicated the inversion parameter δ , i.e., (Mn_{1- δ} Fe δ)^{tet}[Mn δ Fe_{2- δ}]^{oct}O₄, to be higher than the 20%, typically quoted as the equilibrium value.²² As the particle size increased, δ decreased from 62.9 ± 1.8% to 54.2 ± 2.3%. From Fig. 3, it is observed that the highest δ corresponds to both the lowest *T_N* and the highest molar concentration of NaOH. The latter correlates directly with NP growth rate. This trend is in agreement with earlier findings in MnFe₂O₄ films.²⁹ The cation valence strongly contributes to the exchange interaction. From the linear fitting of the Mn and Fe *K* edge XANES, using a combination of spectra collected from binary oxide standards, we measured that more than 93% of Fe ions are trivalent in NP samples. A representative best fit to Fe *K* edge XANES are shown in Fig. 2(b). The fitting of the Mn XANES indicated a distribution of ~55% divalent, ~35% trivalent, and ~10% quadrivalent ions. The appearance of quadrivalent Mn indicates the presence of cation defects. MFT approximation of the bulk MnFe₂O₄ (Ref. 30) predicted that a lower inversion parameter would lead to a lower Néel temperature. This is opposite of what we observe experimentally. We believe that modifications are required in applying MFT to ferrite NP systems. For example,

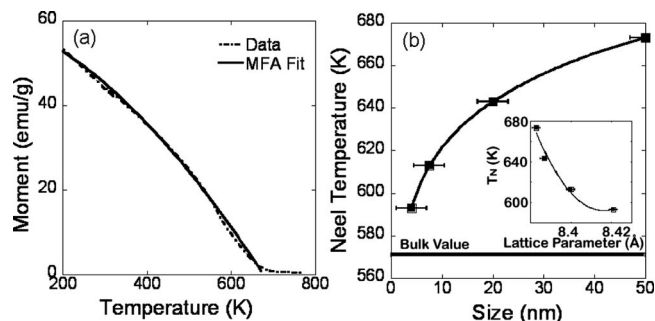


FIG. 1. (a) Thermomagnetic data with best fit from MFT approximation for the 50 nm sample. Data were collected under the application of a 1000 Oe magnetic field. (b) The Néel temperatures determined by MFT fitting of thermomagnetic data plotted against average NP diameters. The inset is a plot of the Néel temperatures as a function of lattice parameter.

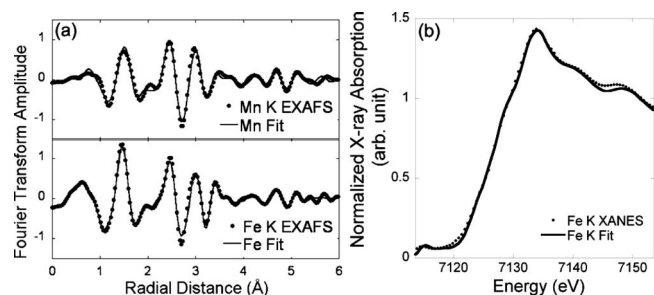


FIG. 2. (a) Real part of the Fourier transformed Fe and Mn *K* edge EXAFS data with best fit data for 7.5 nm diameter Mn-ferrite NP sample. (b) Fe *K* edge XANES data with best linear combination fit for the same sample.

Yafet–Kittel surface spin canting³¹ was not taken into consideration in the determination of molecular field coefficients.³⁰ Although previous researchers reported enhanced T_N as particle size is reduced,^{6,8} we demonstrated that T_N is not dominated by particle size or surface properties but rather by cation inversion and its effect upon exchange. By increasing the growth rate the particles experience higher inversion parameters leading to a lower T_N . The effect of increasing particle growth rate is akin to “quenching in” cation disorder, which has been widely reported in pulsed laser deposited ferrite films.³² From the EXAFS fitting results, a higher mean square radial displacement relative to Mn ions was measured, consistent with there being multiple oxidation states within the structure. Increasing the valence of Mn ions from +2, +3, to +4 would lower the overall magnetization and introduce a Jahn–Teller distortion local to trivalent Mn ions. These effects collectively result in lattice contractions, decreased oxygen parameters, increased inversion parameters, increased exchange interactions, and ultimately in an enhanced T_N . These results contradict previously published reports of trends between Néel temperature and particle size and demonstrate the dominance of cation inversion in determining the strength of superexchange interactions and Néel temperature in ferrite systems. The particle surface chemistry, structure, magnetic spin configuration, and/or finite scaling, play secondary roles.

This research was supported by the National Science Foundation under Grant No. DMR 0400676 and the Office

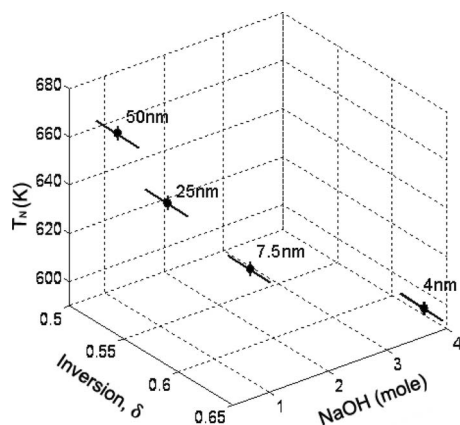


FIG. 3. Néel temperature (T_N) vs inversion parameter δ as described by $(\text{Mn}_{1-\delta}\text{Fe}_\delta)^{\text{tet}}[\text{Mn}_\delta\text{Fe}_{2-\delta}]^{\text{oct}}\text{O}_4$ and molar concentration of NaOH solution used in chemical processing of NPs. Error bars, plotted on the inversion parameters and Néel temperatures, reflect the uncertainty in the measurements and modeling analyses. The measured particle diameters for each sample are denoted aside each data point.

of Naval Research under Grant No. N00014-05-10349 and was performed, in part, at the Department of Energy supported National Synchrotron Light Source (Brookhaven National Laboratory, Upton, NY). At the time of this research, Ms. Kailin Hsu was a student attending the Walt Whitman High School of Bethesda, Maryland.

- ¹D. G. Mitchell, *J. Magn. Reson. Imaging* **7**, 1 (1997).
- ²*Scientific and Clinical Applications of Magnetic Carriers*, edited by U. Häfeli, W. Schütt, J. Teller, and M. Zborowski (Plenum, New York, 1997).
- ³J. F. Hochepeid, P. Bonville, and M. P. Pileni, *J. Phys. Chem. B* **104**, 905 (2000).
- ⁴S. A. Morrison, C. L. Cahill, E. E. Carpenter, S. Calvin, R. Swaminathan, M. E. McHenry, and V. G. Harris, *J. Appl. Phys.* **95**, 6392 (2004).
- ⁵M. A. Willard, L. K. Kurihara, E. E. Carpenter, S. Calvin, and V. G. Harris, *Int. Mater. Rev.* **49**, 125 (2004).
- ⁶Z. X. Tang, C. M. Sorensen, K. J. Kaubunde, and G. C. Hadjipanayis, *Phys. Rev. Lett.* **67**, 3602 (1991).
- ⁷P. J. van der Zaag, A. Noordermeer, M. T. Jonson, and P. F. Bongers, *Phys. Rev. Lett.* **68**, 3112 (1992).
- ⁸G. U. Kulkarni, K. R. Kannan, T. Arunarkavalli, and C. N. R. Rao, *Phys. Rev. B* **49**, 724 (1994).
- ⁹J. P. Chen, C. M. Sorensen, K. J. Klabunde, G. C. Hadjipanayis, E. Devlin, and A. Kostikas, *Phys. Rev. B* **54**, 9288 (1996).
- ¹⁰D. J. Fatemi, V. G. Harris, V. M. Browning, and J. P. Kirkland, *J. Appl. Phys.* **83**, 6867 (1998); D. J. Fatemi, V. G. Harris, M. X. Chen, S. K. Malik, W. B. Yelon, G. J. Long, and A. Mohan, *ibid.* **85**, 5172 (1999).
- ¹¹S. A. Oliver, V. G. Harris, H. Hamdeh, and J. C. Ho, *Appl. Phys. Lett.* **76**, 2761 (2000).
- ¹²C. N. Chinnasamy, A. Narayanasamy, N. Ponpandian, K. Chattopadhyay, K. Shinoda, B. Jeyadevan, K. Tohji, K. Nakatsuka, T. Furubayashi, and I. Nakatani, *Phys. Rev. B* **63**, 184108 (2001).
- ¹³C. N. Chinnasamy, A. Narayanasamy, N. Ponpandian, R. J. Joseyphus, B. Jeyadevan, K. Tohji, and K. Chattopadhyay, *J. Magn. Magn. Mater.* **238**, 281 (2002).
- ¹⁴N. Ponpandian, A. Narayanasamy, C. N. Chinnasamy, N. Sivakumar, J.-M. Grenèche, K. Chattopadhyay, K. Shinoda, B. Jeyadevan, and K. Tohji, *Appl. Phys. Lett.* **86**, 192510 (2005).
- ¹⁵K. Giri, E. M. Kirkpatrick, P. Moongkhamklang, S. A. Majetich, and V. G. Harris, *Appl. Phys. Lett.* **80**, 2341 (2002).
- ¹⁶Z. X. Tang, J. P. Chen, C. M. Sorensen, K. J. Klabunde, and G. C. Hadjipanayis, *Phys. Rev. Lett.* **68**, 3114 (1992).
- ¹⁷Z. J. Zhang, Z. L. Wang, B. C. Chakoumakos, and J. S. Yin, *J. Am. Chem. Soc.* **120**, 1800 (1998).
- ¹⁸M. Muroi, R. Street, and P. G. McCormick, *Phys. Rev. B* **63**, 184414 (2001).
- ¹⁹L. Chao and Z. J. Zhang, *Chem. Mater.* **13**, 2092 (2001).
- ²⁰C. N. Chinnasamy, A. Yang, S. D. Yoon, K. Hsu, M. D. Shultz, E. E. Carpenter, S. Mukerjee, C. Vittoria, and V. G. Harris, *J. Appl. Phys.* **101**, 09M509 (2007).
- ²¹P. J. van der Zaag, V. A. M. Brabers, M. T. Johnson, A. Noordermeer, and P. F. Bongers, *Phys. Rev. B* **51**, 12009 (1995).
- ²²J. Smit and H. P. J. Wijn, *Ferrites* (Wiley, New York, 1959).
- ²³B. Ravel and M. Newville, *J. Synchrotron Radiat.* **12**, 537 (2005).
- ²⁴V. G. Harris, N. C. Koon, C. M. Williams, Q. Zhang, M. Abe, and J. Kirkland, *Appl. Phys. Lett.* **68**, 2082 (1996).
- ²⁵S. Calvin, E. E. Carpenter, B. Ravel, V. G. Harris, and S. A. Morrison, *Appl. Phys. Lett.* **81**, 3828 (2002); *Phys. Rev. B* **66**, 224405 (2002).
- ²⁶J. J. Rehr, S. I. Zabinsky, and R. C. Albers, *Phys. Rev. Lett.* **81**, 3828 (2002).
- ²⁷A. Yang, V. G. Harris, S. Calvin, X. Zuo, and C. Vittoria, *IEEE Trans. Magn.* **40**, 2802 (2004).
- ²⁸G. A. Samara and A. A. Giardini, *Phys. Rev.* **186**, 577 (1969).
- ²⁹X. Zuo, F. Yang, R. Mafhoum, R. Karim, A. Tebano, G. Balestrino, V. G. Harris, and C. Vittoria, *IEEE Trans. Magn.* **40**, 2811 (2004).
- ³⁰G. Dionne, *J. Appl. Phys.* **63**, 3777 (1988).
- ³¹J. M. D. Coey, *Phys. Rev. Lett.* **27**, 1140 (1971).
- ³²X. Zuo, A. Yang, S. D. Yoon, J. A. Christodoulides, V. G. Harris, and C. Vittoria, *Appl. Phys. Lett.* **87**, 152505 (2005); A. Yang, Z. Chen, D. A. Arena, J. Kirkland, C. Vittoria, and V. G. Harris, *ibid.* **86**, 252510 (2005); A. Yang, X. Zuo, C. Vittoria, and V. G. Harris, *IEEE Trans. Magn.* **42**, 2870 (2006); A. Yang, Z. Chen, A. Geiler, X. Zuo, D. Haskel, E. Kravtsov, C. Vittoria, and V. G. Harris, *Appl. Phys. Lett.* **93**, 052504 (2008).